

# Conditional Density Estimations from Privacy-Protected Data

Yifei Xiong<sup>1</sup> , Nianqiao P. Ju<sup>2\*</sup>, Sanguo Zhang<sup>1</sup>

<sup>1</sup>University of Chinese Academy of Sciences

<sup>2</sup>Department of Statistics, Purdue University

## Abstract

Many modern statistical analysis and machine learning applications require training models on sensitive user data. Differential privacy provides a formal guarantee that individual-level information about users does not leak. In this framework, randomized algorithms inject calibrated noise into the confidential data, resulting in privacy-protected datasets or queries. However, restricting access to only the privatized data during statistical analysis makes it computationally challenging to perform valid inferences on parameters underlying the confidential data. In this work, we propose simulation-based inference methods from privacy-protected datasets. Specifically, we use neural conditional density estimators as a flexible family of distributions to approximate the posterior distribution of model parameters given the observed private query results. We illustrate our methods on discrete time-series data under an infectious disease model and on ordinary linear regression models. Illustrating the privacy-utility trade-off, our experiments and analysis demonstrate the necessity and feasibility of designing valid statistical inference procedures to correct for biases introduced by the privacy-protection mechanisms.

## 1 Introduction

**Motivation.** Many AI systems require collecting and training on massive amounts of personal information (such as income, disease status, location, purchase history, etc). Despite unprecedented data collection efforts, by companies, governments, researchers, and other agencies, oftentimes the data collectors have to lock the data inside their own database due to privacy concerns. Differential privacy (DP) provides a mathematical definition for privacy-protection of individual’s data. Under this framework, privacy-protecting procedures (i.e. DP-algorithms) have enabled data collectors, such as tech companies, the US Census Bureau, and social scientists, to share research data in a wide variety of settings while protecting the privacy of individual users. Privacy researchers typically collect some confidential data and then inject calibrated random noise into the confidential data to achieve the desired levels of privacy protection. Some algorithms aim for DP data analysis, resulting in DP optimizations (Arora et al., 2023; Bassily et al., 2021), approximations (Chaudhuri et al., 2013; Bie et al., 2023), or predictions (Rho et al., 2023); while other algorithms produce DP datasets (or descriptive statistics), which enables data sharing across research teams and entities. Examples of the later includes the 2020 US Census (Abowd et al., 2022; Gong et al., 2022; Drechsler, 2023) and Facebook URL dataset (Evans and King, 2023). Our work focuses on this data sharing regime and complex models (e.g. continuous-time Markov jump processes).

While the DP data sharing regime corrupts confidential information in order to satisfy privacy, since the probabilistic design of such mechanisms can be publicly known, in principle, analysts can still conduct reliable estimation and uncertainty quantification by accounting for

---

\*Corresponding author: nianqiao@purdue.edu

bias and noises introduced during privatization. In practice, however, valid inference based on privatized data is a challenge that requires revision of existing statistical methods that were designed originally for confidential data. Even for well-understood procedures such as ordinary linear regression and generalized linear models, adding the extra layer of privacy protection has introduced new theoretical and methodological questions in statistics (Cai et al., 2021; Alabi and Vadhan, 2022; Li et al., 2023; Barrientos et al., 2019)

In many applications, even the confidential data likelihoods functions are intractable or time consuming to compute. Accounting for privacy noise on top of model complexity is a formidable challenge. Without developing valid inference procedures under this regime, we either make biased estimations or have to restrict ourselves to simple models. In this work, we propose methods to estimate parameters of complex models underlying privacy-protected data.

**Related works.** A fast-growing literature has grown on the topic of statistical inference under differential privacy. We point out several Bayesian inference methods from privatized data. Markov Chain Monte Carlo (MCMC) methods have been proposed in some specific models and priors, such as exponential family distributions (Bernstein and Sheldon, 2018) and Bayesian linear regression (Bernstein and Sheldon, 2019). As for generic algorithms, Ju et al. (2022) proposed a data-augmentation MCMC strategy to overcome the intractable marginal likelihood resulting from privatization, and Gong (2022) derived point estimates of the posterior distribution using the Expectation-Maximization algorithm. Several frequentist inference methods have also been developed. Karwa et al. (2015) employed a parametric bootstrap method to construct confidence intervals for the model parameters of the log-linear model. Awan and Wang (2023) proposes simulation-based inference methods for hypothesis testing and confidence intervals.

To the best of our knowledge, only two papers (Waites and Cummings, 2021; Su et al., 2023) have incorporated normalizing flows (Kobyzev et al., 2020; Papamakarios et al., 2021) and DP, and both works design DP-versions of normalizing flow. In contrast, our work uses flow-based methods as a neural density estimation tool to analyze DP-protected data.

**Our contributions.** In this work, we propose several likelihood-free inference methods that make statistical inferences from privacy-protected data. Specifically, we use sequential neural density estimation methods, which use neural networks as a flexible family of distributions to approximate the private data posterior distribution. Unlike existing methods for private data, these simulation-based methods only requires simulations from a generative model for confidential data. We demonstrate the efficiency and utility of our methods on an infectious disease model and ordinary linear regression, using both synthetic and real disease outbreaks data. For the former, we also propose a mechanism for DP release of the infection curve.

## 2 Background and challenges

Let  $\theta \in \Theta$  be the model parameter and  $x = (x_1, \dots, x_n) \in \mathbb{X}^n$  represent the confidential database, containing a total of  $n$  records. We model the database with some likelihood function  $f(x | \theta)$ . This is a confidential data model, which can be a ‘simulator’, whose likelihood can be impossible to compute. Before adding privacy, suppose we have observed some sample  $x^o$ , our inference objective is to perform inference on the posterior distribution  $\pi(\theta | x^o) \propto p(\theta) f(x^o | \theta)$  where  $p(\theta)$  is a prior. Our work study posterior inference under the constraint of DP, where we learn about  $x$  through some DP query result  $s_{dp}$ .

**Differential privacy.** Given some confidential data  $x$ , let  $\eta$  be a randomized algorithm for producing a ‘differentially private statistic’  $s_{dp}$  from  $x$ . We use also  $\eta(s_{dp} | x)$  to denote the conditional density of the private output given confidential  $x$ .

Intuitively, privacy protection is achieve when perturbing one individual’s response in the dataset have only a small change on the outcome of the algorithm. We formally present the definition of  $\epsilon$ -DP from Dwork et al. (2006), where neighboring databases induce ‘close’ distributions on  $s_{dp}$ .

**Definition 1** ( $\epsilon$ -DP). A randomized algorithm  $\eta$  is said to satisfy  $\epsilon$ -DP if for all possible values of  $s_{dp}$  and for all pairs of ‘neighboring’ databases  $(x, x') \in \mathbb{X}^n \times \mathbb{X}^n$ , which are databases differing by just one record [denoted by  $d(x, x') \leq 1$ ], the following probability ratio is bounded:

$$\frac{\int_A \eta(s_{dp} | x) ds_{dp}}{\int_A \eta(s_{dp} | x') ds_{dp}} \leq \exp(\epsilon), \quad \forall A \subseteq \text{Image}(\eta). \quad (1)$$

The parameter  $\epsilon$  is referred to as the *privacy loss budget*, and it plays a pivotal role in determining the extent to which  $s_{dp}$  discloses information about  $x$ : Larger values of  $\epsilon$  correspond to reduced privacy guarantees, whereas  $\epsilon = 0$  signifies perfect privacy.

Output perturbation is a popular class of DP mechanism, where privacy is achieved by first computing a function  $s : \mathbb{X}^n \rightarrow \mathbb{S}$  (such as mean, median, histogram, contingency tables (Giddens and Liu, 2023)) of the database and then releasing  $s(x)$  with some noise. Reaching  $\epsilon$ -DP usually requires finite sensitivity of  $s$ .

**Definition 2** (Global sensitivity (Nissim et al., 2007)). The  $L_p$  sensitivity of a function  $s$ , denoted  $\Delta_p(s)$ , is the maximum  $L_p$ -norm change in the function’s value between neighboring databases  $x$  and  $x'$ , namely

$$\Delta_p(s) = \max_{d(x, x')=1} \|\nu(x) - \nu(x')\|_p.$$

The Laplace mechanism is a popular privacy protection technique.

**Proposition 3** (Laplace mechanism (Dwork et al., 2006)). *For a real-valued query  $\nu : \mathbb{X}^n \rightarrow \mathbb{R}$ , adding Laplace noise with parameter  $\Delta_1(s)/\epsilon$  achieve  $\epsilon$ -DP.*

Chaudhuri et al. (2013) provides a multivariate version of the Laplace mechanism. Other mechanisms include exponential mechanism and Gaussian mechanism (Liu, 2018). There are also relaxations of  $\epsilon$ -DP, such as  $(\epsilon, \delta)$ -DP and Gaussian DP (Dong et al., 2022).

Since many queries are embedded in lower dimensional manifold spaces than the confidential data, this can facilitate efficient computations. In Section 3.3, we leverage the low dimensionality of  $s_{dp}$  by incorporating quasi Monte Carlo techniques.

**Intractable likelihood and posterior.** A key challenge with data analysis on privatized data is the intractable likelihood.

$$f(s_{dp} | \theta) = \int_{\mathbb{X}^n} f(x | \theta) \eta(s_{dp} | \theta) dx. \quad (2)$$

When the confidential data likelihood  $f(x | \theta)$  can be evaluated, Ju et al. (2022) proposed a data-augmentation MCMC algorithm to approximate the private data posterior

$$\pi(\theta | s_{dp}) \propto f(s_{dp} | \theta) p(\theta). \quad (3)$$

The data augmentation strategy circumvents the intractability of Eq.(2) by working with the joint posterior distribution  $\pi(\theta, x | s_{dp}) \propto f(x | \theta) p(\theta) \eta(s_{dp} | \theta)$  instead of the marginal posterior in Eq.(3).

In this work, we study the challenging scenarios when the confidential likelihood is no longer analytically tractable or is time-consuming to compute. This situation is ‘triple intractable’, as there are three levels of intractability, in  $f(x | \theta)$ ,  $f(s_{dp} | \theta)$ , and  $\pi(\theta | s_{dp})$ .

**Likelihood-free inference.** For complex confidential data generating processes (Gourieroux et al., 1993; Brehmer et al., 2020), several studies have trained conditional density estimators to perform likelihood-free inference. Recent advancements have embraced the use of neural networks, in particular, normalizing flows (Dinh et al., 2016; Papamakarios et al., 2017; Durkan et al., 2019; Papamakarios et al., 2021) as a highly flexible family of conditional densities.

We review the idea of neural density approximations on the confidential data posterior. Using the variational family  $\{q_\phi(\theta | x)\}$  to approximate a target distribution  $\pi(\theta | x^o)$ , we can set up a loss function  $\ell(\phi) = -\sum_{i=1}^N \log q_\phi(\theta^{(i)} | x^{(i)})$ , where the training data  $\{(\theta^{(i)}, x^{(i)})\}_{i=1}^N$  are sampled from the joint probability density  $f(\theta, x) = p(\theta)f(x | \theta)$ . The loss function  $\ell(\phi)$  is a sample-based approximation of  $\mathbb{E}_{(\theta, x) \sim f} [-\log q_\phi(\theta | x)]$ , which is known as the (negative) evidence lower bound in the variational inference literature (Blei et al., 2017). The objective is equivalent to minimizing the Kullback-Leibler divergence between the target and the variational family  $q_\phi$ .

Recognizing that it can be inefficient to propose from the joint model  $f(\theta, x)$ , we can design sequential training procedures (Papamakarios and Murray, 2016; Lueckmann et al., 2017; Greenberg et al., 2019) that gradually improves  $q_\phi$  by using the current approximation as the proposal distribution for the next round. Other neural density estimation approaches include approximating the likelihood functions (Papamakarios et al., 2019) or likelihood ratios (Miller et al., 2022). We refer readers to Cranmer et al. (2020); Lueckmann et al. (2021) for systematic reviews on the topic.

### 3 Methods

We aim to train conditional density estimators to estimate the private data posterior  $\pi(\theta | s_{dp})$ . We consider two complementary approaches: 1) approximate the private data marginal likelihood  $p(s_{dp} | \theta)$  and 2) approximate  $\pi(\theta | s_{dp})$  directly.

#### 3.1 Private data likelihood estimation

Our first strategy is a neural likelihood estimator  $q_\phi(s_{dp} | \theta)$  to approximate the private data marginal likelihood  $f(s_{dp} | \theta)$ . When training  $q_\phi(s_{dp} | \theta) \approx f(s_{dp} | \theta)$ , we aim to minimize their average KL divergence under the prior  $p(\theta)$ , corresponding to

$$\hat{\phi} = \arg \min \mathbb{E}_{p(\theta)} [\mathcal{D}_{KL} (p(s_{dp} | \theta) \| q_\phi(s_{dp} | \theta))] . \quad (4)$$

Eq. (4) is equivalent to  $\mathbb{E}_{\theta, s_{dp}} [-\log q_\phi(s_{dp} | \theta)]$  up to a constant independent of  $\phi$ , where the expectation is taken with respect to the prior and the private data generating process  $(\theta, s_{dp}) \sim p(\theta) \cdot f(s_{dp} | \theta)$ . We can also integrate with respect to the confidential data generating process, with objective function

$$\ell_{PLE}(\phi) = \mathbb{E}_{p(\theta, x)} \left[ - \int_{\mathbb{S}} \eta(s_{dp} | x) \log q_\phi(s_{dp} | \theta) ds_{dp} \right] . \quad (5)$$

We defer derivation details to the appendix.

When the primary inference goal is the maximum likelihood estimator, one can approximate it with  $\hat{\theta}_{MLE} = \arg \max_{\theta} q_\phi(s_{dp} | \theta)$ . Under the Bayesian paradigm, the posterior approximation to Eq. (3) can be  $\hat{\pi}_{PLE}(\theta) \propto p(\theta)q_\phi(s_{dp} | \theta)$ . Quantities such as posterior median, mean, and credible regions can be estimated accordingly.

#### 3.2 Private data posterior estimation

We can also approximate the private data posterior  $\pi(\theta | s_{dp})$  in Eq. (3) directly, bypassing the synthetic likelihood step, with a neural posterior estimator  $q_\phi(\theta | s_{dp})$ . Learning  $q_\phi(\theta | s_{dp}) \approx \pi(\theta | s_{dp})$ , we can minimize their KL divergence.

$$\mathcal{D}_{KL} (\pi(\theta | s_{dp}) \| q_\phi(\theta | s_{dp})) = \mathbb{E}_{\pi(\theta | s_{dp})} \left[ \log \frac{\pi(\theta | s_{dp})}{q_\phi(\theta | s_{dp})} \right] . \quad (6)$$

We can write the loss function as

$$\ell_{\text{PPE}}(\phi) = \mathbb{E}_{p(\theta, x)} \left[ - \int_{\mathbb{S}} \eta(s_{\text{dp}} \mid x) \log q_{\phi}(\theta \mid s_{\text{dp}}) ds_{\text{dp}} \right]. \quad (7)$$

Many Bayesian problems assume an uninformative prior  $p(\theta)$ , which covers the parameter space instead of concentrating on high density regions of the posterior. As a result, a naive Monte Carlo strategy to approximate the expectation in Eq.(7) will be inefficient. Similar to importance sampling, where one utilize a proposal distribution  $\tilde{p}(\theta)$  to reduce variance during numerical integration, we can rewrite Eq.(7) as an expectation with respect to some proposal distribution  $\tilde{q}$ . [Greenberg et al. \(2019\)](#) proposed the Automatic Posterior Transformation (APT) method, with

$$\tilde{q}_{\phi}(\theta \mid s_{\text{dp}}) := q_{\phi}(\theta \mid s_{\text{dp}}) \frac{\tilde{p}(\theta)}{p(\theta)} \frac{1}{Z(s_{\text{dp}}, \phi)},$$

where  $Z(s_{\text{dp}}, \phi)$  is a normalization constant and can be estimated as  $\sum_{\theta' \in \Theta} q_{\phi}(\theta' \mid s_{\text{dp}})/p(\theta')$ ,  $\theta' \sim \tilde{p}(\theta)$  using importance sampling. In this case, the loss function based on APT is

$$\ell_{\text{PPE-A}}(\phi) = \mathbb{E}_{\tilde{p}(\theta, x)} \left[ - \int_{\mathbb{S}} \eta(s_{\text{dp}} \mid x) \log \tilde{q}_{\phi}(\theta \mid s_{\text{dp}}) ds_{\text{dp}} \right]. \quad (8)$$

This APT-based objective function will be useful for the sequential training we introduce in Section 3.4.

### 3.3 Nested RQMC estimators

Both loss functions in Eq.(5) and (8) are double integrals, where the outer integral is an expectation with respect to some proposal distribution  $\tilde{p}$  and the inner integral involves the privacy mechanism  $\eta$  and the neural estimator  $q_{\phi}$ . We can inspect their general forms

$$\ell(\phi) = -\mathbb{E}_{\tilde{p}(\theta, x)} \left[ \int_{\mathbb{S}} \eta(s_{\text{dp}} \mid x) g(s_{\text{dp}}, \theta) ds_{\text{dp}} \right]. \quad (9)$$

Here  $g(s_{\text{dp}}, \theta) = \log \tilde{q}_{\phi}(\theta \mid s_{\text{dp}})$  for PPE-A and  $g(s_{\text{dp}}, \theta) = \log q_{\phi}(s_{\text{dp}} \mid \theta)$  for PLE.

With iid samples from the joint density  $\{(\theta^{(i)}, x^{(i)})\}_{i=1}^N \sim \tilde{p}(\theta, x) = \tilde{p}(\theta)f(x|\theta)$ , we can unbiasedly approximate Eq.(9) with

$$\hat{\ell}(\phi)^{\text{MC}} = - \sum_{i=1}^N \left[ \int_{\mathbb{S}} \eta(s_{\text{dp}} \mid x^{(i)}) g(s_{\text{dp}}, \theta^{(i)}) ds_{\text{dp}} \right]. \quad (10)$$

The inner integrals  $I(\theta, x) = \int \eta(s_{\text{dp}} \mid x) g(s_{\text{dp}}, \theta) ds_{\text{dp}}$  can be approximated with standard Monte Carlo integration techniques, as popular DP mechanisms such as Laplace, Gaussian, and Exponential can be easily simulated. For MC strategies with  $M$  samples, the root-mean-squared-error (RMSE) of  $I(\theta, x)$  approximations are typically at the order of  $\mathcal{O}(1/\sqrt{M})$ .

In many applications, the DP query result  $s_{\text{dp}}$  is a private descriptive statistic of  $x$ , which means  $s_{\text{dp}}$  is embedded in a low-dimensional space  $\mathbb{S}$  with  $r = \dim(\mathbb{S}) \leq \dim(\mathbb{X}^n)$ . Let  $u \sim \mathcal{U}[0, 1]^r$  be a random number from the  $r$ -dimensional hypercube, fixing  $x$ , we can write the mechanism by  $\tau : [0, 1]^r \rightarrow \mathbb{S}$  with  $\tau(u; s(x))$ .

We can leverage randomized quasi-Monte Carlo (RQMC) ([Owen, 1997](#); [L'Ecuyer, 2018](#)) to efficiently integrate over the low-dimensional space and achieve favorable convergence rates for numerical integration. RQMC generates a low-discrepancy sequence  $\{v^{(1)}, \dots, v^{(M)}\} \subset [0, 1]^r$  to achieve the estimator

$$\hat{I}_{\theta, x}^{\text{RQMC}} = \frac{1}{M} \sum_{j=1}^M g(\tau(v^{(j)}; x), \theta) := \frac{1}{M} \sum_{j=1}^M \tilde{g}_{\theta, x}(v^{(j)}) \quad (11)$$

In addition to being unbiased, the RQMC estimator also has RMSE compared to MC estimators. The  $\star$ -discrepancy of the point set  $\{v^{(1:M)}\}$ , denoted by  $D^*(v^{(1:M)})$  is of the order  $\mathcal{O}(M^{-1}(\log M)^r) = \mathcal{O}(M^{-1+\delta})$  for a positive constant  $\delta$ . If our neural approximation family  $\tilde{g}_{\theta,x}(\cdot)$  has bounded Hardy-Krause variation  $V_{\text{HK}}[\tilde{g}_{\theta,x}(\cdot)]$  (Aistleitner et al., 2017), then, according to Basu and Owen (2016), the variance of the RQMC estimator in Eq.(11) satisfies

$$\text{Var}(\hat{I}_{\theta,x}^{\text{RQMC}}) \leq V_{\text{HK}}^2(\tilde{g}_{\theta,x})(D^*)^2 = \mathcal{O}(M^{-2+\delta}). \quad (12)$$

Thus the RMSE of RQMC is of the order  $\mathcal{O}(M^{-1+\delta/2})$ , achieving faster convergence than an MC estimator. We verify this improvement in convergence from the RQMC estimator on the SIR model and linear regression example with the neural spline flow approximation family (Durkan et al., 2019), in Fig. 1.

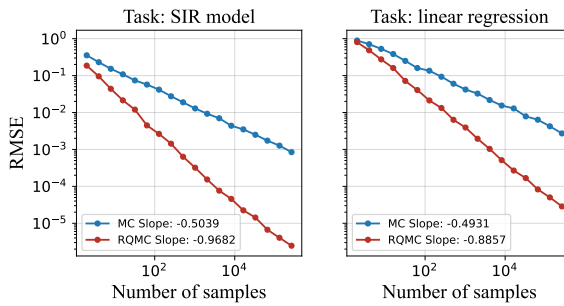


Figure 1: Rate of convergence of MC and RQMC.

### 3.4 Sequential neural estimations

This section discusses our sequential neural approximation methods on privacy-protected data. We summarize the Sequential Private Posterior Estimation (SPPE) algorithm in Algo.1 and the Sequential Private Likelihood Estimation (SPLE) in Algo.2.

---

#### Algorithm 1 Sequential private-data posterior estimation

---

**Input:** observed privatized summary statistics  $s_{\text{dp}}^o$ , neural estimation family  $q_\phi(\theta | s_{\text{dp}})$ , and confidential data simulator  $f(x | \theta)$ .  
**Initialization:** set  $\tilde{p}_0(\theta) = p(\theta)$ , simulated data filtration  $\mathcal{D}_0 = \{\}$   
**for**  $r = 1, 2, \dots, R$  **do**  
    Sample  $\{\theta^{(i)}\}_{i=1:N}$  from  $\tilde{p}_{r-1}(\theta)$ .  
    Simulate  $x^{(i)} \sim f(\cdot | \theta^{(i)})$  for each  $i$ .  
    Update filtration  $\mathcal{D}_r = \mathcal{D}_{r-1} \cup \{(\theta^{(i)}, x^{(i)})\}_{i=1:N}$ .  
    Update  $\phi \leftarrow \arg \min_\phi \hat{\ell}_{\text{PPE-A}}(\phi)$  using  $\hat{I}^{\text{RQMC}}$  (11) on  $\mathcal{D}_r$ .  
    Set proposal  $\tilde{p}_r(\theta) = q_\phi(\theta | s_{\text{dp}}^o)$   
**end for**  
**return**  $\hat{\pi}(\theta | s_{\text{dp}}^o) = \tilde{p}_R(\theta)$ .

---

Our methods refine the normalizing flows  $q_\phi$  to approximate the target distributions by iteratively minimizing the loss functions taking the general form in Eq.(9). In Eq.(9), using a proposal distribution  $\tilde{p}(\theta, x)$  that overlaps more with the joint posterior distribution  $\pi(\theta, x | s_{\text{dp}})$  is more efficient than simulation from the prior  $p(\theta)f(x | \theta)$ , in terms of variance reduction for Monte Carlo integration. To this end, we sequentially train the neural density estimators: after round  $r$ , the posterior approximation  $\hat{q}^{(r)}(\theta) \approx \pi(\theta | s_{\text{dp}})$  becomes a proposal distribution in the loss functions  $\ell(\phi)$  for round  $(r+1)$ . This approach can gradually move  $q_\phi$  towards high density regions of the private data posterior, and thus achieve good accuracy with fewer samples from the confidential data simulator.

---

**Algorithm 2** Sequential private-data likelihood estimation

---

**Input:** observed privatized summary statistics  $s_{\text{dp}}^o$ , neural estimation family  $q_\phi(s_{\text{dp}} | \theta)$ , and confidential data simulator  $f(x | \theta)$ .

**Initialization:** set  $\tilde{p}_0(\theta) := p(\theta)$ , simulated data filtration  $\mathcal{D}_0 = \{\}$

**for**  $r = 1, 2, \dots, R$  **do**

- Sample  $\{\theta^{(i)}\}_{i=1}^N$  from  $\tilde{p}_{r-1}(\theta)$ .
- Simulate  $x^{(i)} \sim f(\cdot | \theta^{(i)})$  for each  $i$ .
- Update filtration  $\mathcal{D}_r = \mathcal{D}_{r-1} \cup \{(\theta^{(i)}, x^{(i)})\}_{i=1:N}$ .
- Update  $\phi \leftarrow \arg \min_\phi \hat{\ell}_{\text{PLE}}(\phi)$  using  $\hat{I}^{\text{RQMC}}$  (11) on  $\mathcal{D}_r$
- Set proposal  $\tilde{p}_r(\theta) \propto p(\theta)q_\phi(s_{\text{dp}}^o | \theta)$

**end for**

**return** posterior estimation  $\hat{\pi}(\theta | s_{\text{dp}}^o) = \tilde{p}_R(\theta)$  and likelihood estimation  $\hat{f}_\theta(s_{\text{dp}} | \theta) = q_{\phi^*}(s_{\text{dp}} | \theta)$ .

---

## 4 Applications

Here we illustrate our methods on the susceptible-infected-recovered (SIR) model and linear regression. We include experiments on the Naïve Bayes log-linear model in the Appendix.

### 4.1 SIR model for disease spread

The SIR model is a time-series model that describes how an infectious disease spread in a closed population. It is most often used as a deterministic ordinary differential equation (ODE), but can also be represented by a Markov jump process.

To the best of our knowledge, inference on privacy-protected data with the SIR model has not been studied in the literature. Our proposed methods are particularly suitable for this problem for two reasons. First, our methods are simulation-based and thus are applicable under the ODE model, when other likelihood-based methods can no longer be applied. Second, in the SIR model, low-dimensional summary statistics can be very informative about the model parameters. Then the RQMC methods discussed in Section 3.3 can provide efficiency and accuracy gains when evaluating the loss functions.

We describe a stochastic SIR model in a closed population with  $K$  people. As the disease spreads, individuals progress through the three states: susceptible, infected, and recovered. We use  $S(t)$ ,  $I(t)$ , and  $R(t)$  to denote the number of individuals within each compartment at time  $t$ . We make the following assumptions: (a) individuals are infected at a rate  $\beta \frac{SI}{K}$ , resulting in a decrease of  $S$  by one and an increase of  $I$  by one, (b) infected individuals recover with a rate  $\gamma I$ , leading to a decrease of  $I$  by one and an increase of  $R$  by one. The confidential data likelihood of this continuous-time Markov jump process proves hard to compute. Our goal is to infer the infection and recovery rates  $\theta = (\beta, \gamma)$ , under initial conditions  $(S, I, R) = (K - 1, 1, 0)$ .

**Privatizing the infection curve.** We propose a mechanism to publish privatized data about the infection process. This algorithm adds calibrated noise to the SIR process, protecting individual's infection status while allowing analysts to make inference about population parameters  $(\beta, \gamma)$ . At each time, the proportion of infected individuals is  $I(t)/K$ . We shall privatize this infection trajectory.

**Proposition 4.** *Consider a sequence of  $L$  points in the time interval  $[0, T]$ , our privatized query can be  $s_{\text{dp}} = (s_1, \dots, s_L)$  where each  $s_i \sim \text{Binomial}\left(n, \frac{I(t_i) + m}{K + 2m}\right)$  independently. The mechanism generating  $s_{\text{dp}} = (s_1, \dots, s_L)$  satisfies  $\epsilon$ -DP, with  $\epsilon = \frac{n}{m}L$ .*

Here  $s_{\text{dp}}$  is a differential private time series, reflecting the speed of disease spread in a population.

**Experiments on synthetic data.** We illustrate the performance of SPPE and SPLE on synthetic privatized SIR model data. The data generating parameters are set to emulate a measles outbreak. We describe prior specifications and implementation details in the appendix.

Figure 2 describes convergence of the posterior approximations  $\hat{\pi}(\theta | s_{dp}^o)$  and compare our results with Sequential Monte Carlo Approximate Bayesian Computations (SMC-ABC) (Beaumont et al., 2009). SMC-ABC is chosen as the base line comparison as it aims to exactly recover the posterior without resorting to variational approximations. We run the SMC-ABC method with up to  $5 \times 10^5$  simulations. Both SPPE and SPLE quickly adapts to meet the SMC-ABC results, with order of magnitude fewer simulations needed. After the first round of simulations, SPPE is able to identify the high probability region of  $\pi(\theta | s_{dp})$ , while the SPLE posterior is still exploring the parameter space. See SI for the SPLE approximation after  $r = 1$ . After  $r = 5$  rounds, both methods are able to concentrate around the posterior mean and have capture the posterior correlation  $\text{cov}(\beta, \gamma | s_{dp})$ . By inspecting marginal posterior histograms

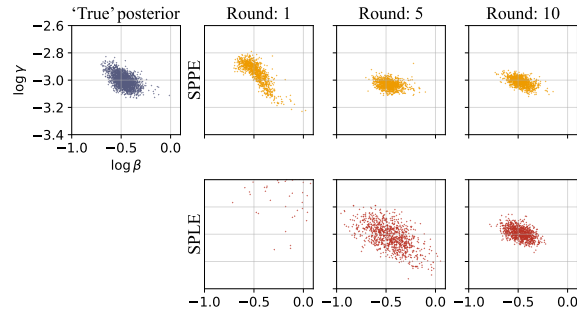


Figure 2: Convergence of sequential posterior estimations given DP-protected infection trajectory under the SIR model. Each round entails  $N = 1000$  simulations. Orange: SPPE; red: SPLE; grey: SMC-ABC.

(See appendix), we find that, in this example, the posterior approximated by SPPE is slightly more concentrated than those from SMC-ABC and SPLE.

To evaluate the performance of our methods, we use the following metrics: (1) MMD (Gretton et al., 2012): maximum mean discrepancy between the neural estimated posteriors and SMC-ABC posterior; (2) C2ST (Lopez-Paz and Oquab, 2016): classifier two sample tests; (3) NLOG: negative log density at true parameters; and (4) LMD: log median distance from simulated to observed  $s_{dp}$ . Smaller values indicate better performance for all four metrics. In Figure 3, we compare the performance of these methods against number of simulation samples/rounds. After Round 5, SPLE and SPPE have similar accuracy. See Appendix for run-time comparisions against SMC-ABC.

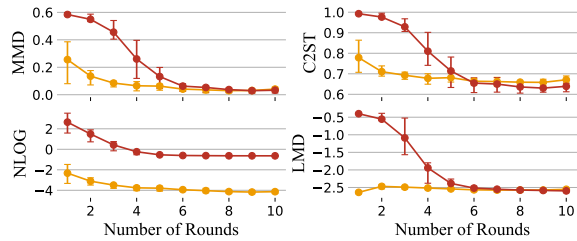


Figure 3: Approximation accuracy by SPPE (orange) and SPLE (red) on the SIR model against number of rounds, the error bars represent the mean with the upper and lower quartiles.

**Real disease outbreaks.** We apply our privacy mechanism and inference methods (SPPE and SPLE) on several real infectious disease outbreaks: influenza, Ebola, and Covid-19. In Fig. 4-A, we compare the posterior distributions  $\pi(\beta, \gamma | s_{dp})$  obtained from SMC-ABC, SPPE,

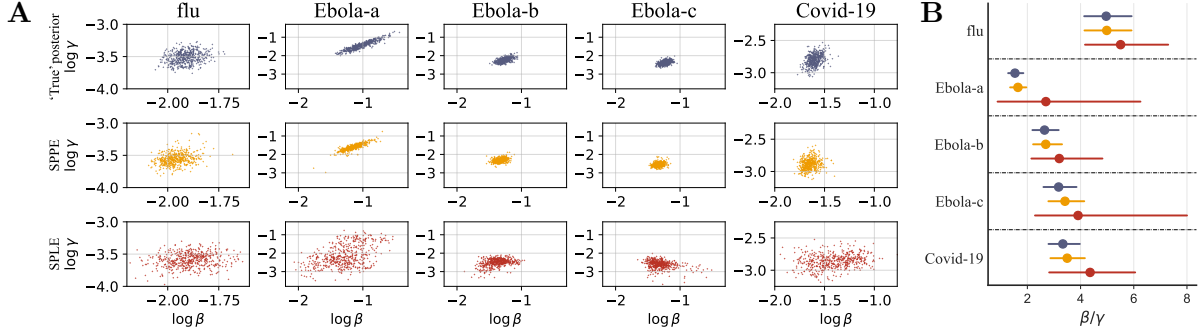


Figure 4: Inference on real infectious disease outbreaks. **A.** Visualization of the posterior distribution given private infection curve on applied to flu, Ebola [in a) Guinea, b) Liberia, and c) Sierra Leone], and Covid-19 in Clark County, Nevada. datasets. **B.** Mean and 95% credible intervals for  $R_0 = \beta/\gamma$  with different methods in each dataset. Grey: SMC-ABC; orange: SPPE; red: SPLE.

and SPLE. The results are similar to synthetic data experiments: when SPPE and SPLE use the same computational resources, the SPPE posterior converges faster than SPLE. In Fig. 4-B, we inspect the 95%-credible interval for the ratio  $R_0 = \beta/\gamma$ , which is known as the basic reproduction number. Our  $R_0$  estimates using privatized data are consistent with common estimates of  $R_0$  for these diseases (Eisenberg, 2020), with the exception of the flu outbreak (which should be modeled by the SI model instead of SIR).

## 4.2 Bayesian linear regression

We demonstrate our methods on a linear regression model, and compare it to existing work on DP regression analysis. We consider linear regression with  $n$  subjects and  $p$  predictors. Denote  $x_0 \in \mathbb{R}^{n \times p}$  as the matrix of predictors excluding the intercept columns, and  $x = (\mathbf{1}_{n \times 1}, x_0)$  represent the matrix that including the intercept. Ordinary linear regression models assume that the outcomes  $y$  satisfy  $y|x_0 \sim \mathcal{N}_n(x\beta, \sigma^2 I_n)$ . Under the constraint of differential privacy, both outcomes  $y$  and predictors  $x_0$  are subject to calibrated noise. In a Bayesian setting, we model the predictors with  $x_{0,i} \sim \mathcal{N}_p(m, \Sigma)$  for  $i = 1, 2, \dots, n$  independently. Our parameter of interest is  $\beta$ , which represents the  $(p+1)$ -dimensional vector of regression coefficients. Our experiments assumes with  $\sigma$ ,  $m$  and  $\Sigma$  are fixed.

	$\beta_0$	$\beta_1$	$\beta_2$
Confidential Posterior given $x$	-2.15 (-2.68, -1.61)	-2.79 (-3.08, -2.50)	-0.83 (-1.08, -0.58)
Naive posterior approximation	-4.63 (-5.04, -4.22)	-6.23 (-6.57, -5.90)	-5.10 (-5.40, -4.79)
SMC-ABC	-0.59 (-2.28, 0.93)	-2.44 (-3.67, -0.38)	0.85 (-0.88, 2.77)
DA-MCMC	-0.62 (-2.50, 0.99)	-2.72 (-3.74, -0.96)	0.54 (-1.06, 2.46)
SPPE	-0.51 (-2.25, 1.07)	-2.40 (-3.61, -0.30)	0.90 (-0.89, 2.85)
SPLE	-0.64 (-2.31, 0.96)	-2.61 (-3.65, -0.98)	0.64 (-0.93, 2.48)

Table 1: Estimated posterior mean and 95% credible intervals for the linear regression example using various methods: SMC-ABC, Data-augmentation MCMC [DA-MCMC, (Ju et al., 2022)], SPPE, SPLE. Here privacy loss budget is set to  $\epsilon = 10$ .

**Private sufficient statistics.** We achieve  $\epsilon$ -DP on confidential data  $(x, y)$  by adding Laplace noise to sufficient statistics. Achieving privacy requires finite  $\ell_1$  sensitivity on confidential data. As a result, before adding noise for privacy, we first need clamp the predictors and response, and then normalize them to take values in  $[-1, 1]$ . Let's denote the clamped

confidential data as  $\tilde{x}$  and  $\tilde{y}$ , respectively. We then define the summary statistics of clamped data as  $\tilde{s} := (\frac{1}{n}\tilde{x}^\top \tilde{y}, \frac{1}{n}\tilde{y}^\top \tilde{y}, \frac{1}{n}\tilde{x}^\top \tilde{x})$ . We have refined the sensitivity analysis of [Ju et al. \(2022\)](#) to  $\Delta(s) = \frac{1}{n}(p^2 + 3p + 3)$ . The privacy summary statistics  $s_{dp}$  is achieved by adding independent Laplace( $0, \Delta_1(\tilde{s})/\epsilon$ ) noise to each entry of  $\tilde{s}$ . This mechanism satisfies  $\epsilon$ -DP, and it is connected to measurement-error models in statistics ([Carroll et al., 1995](#); [Hu et al., 2022](#)). Details of clamping and sensitivity analysis are in the supplementary materials.

**The cost of privacy.** Although it has been a standard practice in many DP work ([Bernstein and Sheldon, 2018, 2019](#); [Ju et al., 2022](#); [Gong, 2022](#)) to achieve finite global sensitivity through clamping, this benefit of privacy protection comes at a cost of accuracy of the subsequent statistical analysis. Biases introduced by measurement errors (privacy noise) and truncation (clamping) are illustrated in Table 1, where we use several methods to compute the private data posterior. First of all, we highlight that it is necessary to design a valid inference procedure after DP data release, as a naive plug-in estimator (plugging in  $s_{dp}$  as  $s$  into the conjugate posterior  $\pi(\theta | s)$ ) gives the wrong posterior. In fact, the clamping step has destroyed the conjugacy properties enjoyed by the confidential data model. Second, achieving privacy protection comes at a cost of estimation accuracy: private data posterior  $\pi(\theta | s_{dp})$  is different from the confidential data posterior  $\pi(\theta | x)$  even under a high loss budget of  $\epsilon = 10$  (small privacy noise) setting. With small privacy noise, data corruption primarily comes from the clamping step. Elevating this censoring bias is still an open problem in DP data analysis, with some recent attempts in [Biswas et al. \(2020\)](#); [Evans et al. \(2019\)](#); [Covington et al. \(2021\)](#).

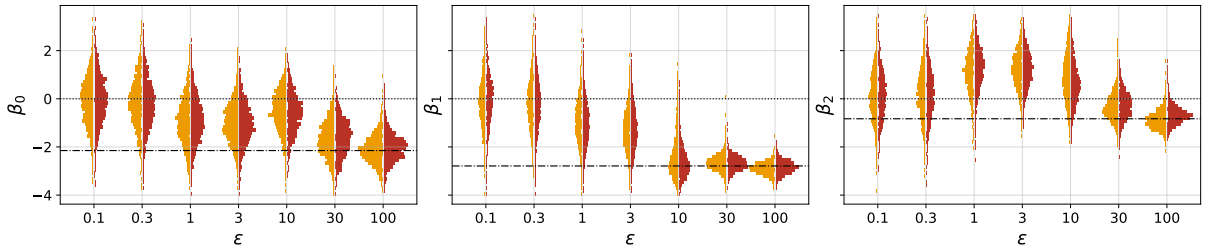


Figure 5: Marginal posterior histograms of  $\theta = (\beta_0, \beta_1, \beta_2)$  given  $s_{dp}$  generated with several levels of privacy loss budget on the same confidential data  $x$ . Orange: SPPE; red: SPLE. The dash-dotted horizontal lines indicate the confidential data posterior means, and the dotted lines indicate prior means.

To further characterize the privacy-utility trade-off, we compare the private data posterior under several levels of privacy loss budget, in Figure 5. The underlying confidential data  $x$  is the same for each  $\epsilon = 0.1, 0.3, 1, 3, 10, 30, 100$ . For each privacy loss level, we simulate one private summary  $s_{dp}(\epsilon)$ , and use SPPE and SPLE to approximate the private data posterior  $\pi(\theta | s_{dp}; \epsilon)$ . The two methods yield very similar posterior inferences. In fact, we use the same confidential data  $x$  as [Ju et al. \(2022\)](#) and the posterior distributions in Figure 5 follow a similar trend with Figure 2 of [Ju et al. \(2022\)](#). For larger privacy loss budget (smaller noise), confidential data is mainly corrupted through clamping and the proposed methods can elevate the effect of this censoring bias, as  $\mathbb{E}(\theta | s_{dp})$  is closer to the confidential data expectation  $\mathbb{E}(\theta | x)$ . As  $\epsilon$  get closer to 0 (larger noise, near perfect privacy), the posterior distribution is more dispersed than the prior distribution, because we have injected too much noise into  $s_{dp}$ .

## 5 Discussion

In this work, we propose two simulation-based inference methods to learn population parameters from privacy-protected data. Leveraging normalizing flows and RQMC, SPPE aims to approximate the posterior-data posterior and SPLE approximates the posterior-data likelihood. Our work contributes to the growing literature on statistical analysis after DP. In particular, the

framework can be applied to complex models, with intractable likelihood functions. The methodology can be especially useful for generative models, which have complex likelihood functions but are easy to simulate from, with the continuous-time SIR infection model being an example of it.

We hope our methods can catalyze DP-protected data sharing between data collectors and analysts. Our experiments and analysis demonstrate the necessity and feasibility of designing valid statistical inference procedures to correct for biases introduced by the privacy-protection mechanisms. We advocate for both an increase of sharing privacy-protected data by collectors and the use of valid inference procedures.

We compare our methods to similar DP data analysis work that focuses on *post processing* of privacy-protected datasets (or their summary statistics). Compared with ABC (Gong, 2022), our method does not reject training samples and hence is more computationally efficient. Compared with DA-MCMC (Ju et al., 2022), our method does not require that the confidential data likelihood can be evaluated easily. These methods require that one can simulate from the prior distribution  $p(\theta)$  and the confidential model  $f(x | \theta)$ . They also all scale linearly with sample size of the confidential database.

We acknowledge limitations of the present work and point out future directions. Using RQMC, our methods leverage low-dimensionality of  $s_{dp}$  as well as the fact that popular DP mechanisms can be efficiently achieved with random number generators. In some applications, such as DP principle component analysis (Chaudhuri et al., 2013), the privacy mechanism is actually intractable to simulate from but its density is easy to evaluate. A novel perspective is to consider the whole process of generating  $s_{dp}$  given  $\theta$  and skipping confidential data simulation as an intermediate step. This corresponds to the case of  $M = 1$  in Eq.(11), as analyzed by Bornn et al. (2017) for similar problems in the context of ABC. Since our method scales linearity in sample size, it might not be ideal for massive datasets, such as the Facebook URL dataset (Evans and King, 2023) which concerns millions of users. It is of interest to develop methods that scales sub-linearly in sample size. Another interesting future direction is the distributed setting (Alparslan et al., 2023), where multiple parties hold parts of the data.

## References

Abowd, J., Ashmead, R., Cumings-Menon, R., Garfinkel, S., Heineck, M., Heiss, C., Johns, R., Kifer, D., Leclerc, P., Machanavajjhala, A., Moran, B., Sexton, W., Spence, M., and Zhuravlev, P. (2022). The 2020 Census Disclosure Avoidance System TopDown Algorithm. *Harvard Data Science Review*, (Special Issue 2). <https://hdsr.mitpress.mit.edu/pub/7evz361i>.

Aistleitner, C., Pausinger, F., Svane, A. M., and Tichy, R. F. (2017). On functions of bounded variation. In *Mathematical Proceedings of the Cambridge Philosophical Society*, volume 162, pages 405–418. Cambridge University Press.

Alabi, D. and Vadhan, S. (2022). Hypothesis testing for differentially private linear regression. *Advances in Neural Information Processing Systems*, 35:14196–14209.

Alparslan, B., Yıldırım, S., and Birbil, I. (2023). Differentially private distributed Bayesian linear regression with MCMC. In Krause, A., Brunskill, E., Cho, K., Engelhardt, B., Sabato, S., and Scarlett, J., editors, *Proceedings of the 40th International Conference on Machine Learning*, volume 202 of *Proceedings of Machine Learning Research*, pages 627–641. PMLR.

Arora, R., Bassily, R., González, T., Guzmán, C. A., Menart, M., and Ullah, E. (2023). Faster rates of convergence to stationary points in differentially private optimization. In *International Conference on Machine Learning*, pages 1060–1092. PMLR.

Awan, J. and Wang, Z. (2023). Simulation-based, finite-sample inference for privatized data.

Barrientos, A. F., Reiter, J. P., Machanavajjhala, A., and Chen, Y. (2019). Differentially private significance tests for regression coefficients. *Journal of Computational and Graphical Statistics*, 28(2):440–453.

Bassily, R., Guzmán, C. A., and Menart, M. (2021). Differentially private stochastic optimization: New results in convex and non-convex settings. In Beygelzimer, A., Dauphin, Y., Liang, P., and Vaughan, J. W., editors, *Advances in Neural Information Processing Systems*.

Basu, K. and Owen, A. B. (2016). Transformations and hardy–krause variation. *SIAM Journal on Numerical Analysis*, 54(3):1946–1966.

Beaumont, M. A., Cornuet, J.-M., Marin, J.-M., and Robert, C. P. (2009). Adaptive approximate bayesian computation. *Biometrika*, 96(4):983–990.

Bernstein, G. and Sheldon, D. R. (2018). Differentially private bayesian inference for exponential families. *Advances in Neural Information Processing Systems*, 31.

Bernstein, G. and Sheldon, D. R. (2019). Differentially private bayesian linear regression. *Advances in Neural Information Processing Systems*, 32.

Bie, A., Kamath, G., and Zhang, G. (2023). Private gans, revisited. *arXiv preprint arXiv:2302.02936*.

Biswas, S., Dong, Y., Kamath, G., and Ullman, J. (2020). Coinpress: Practical private mean and covariance estimation. In Larochelle, H., Ranzato, M., Hadsell, R., Balcan, M., and Lin, H., editors, *Advances in Neural Information Processing Systems*, volume 33, pages 14475–14485. Curran Associates, Inc.

Blei, D. M., Kucukelbir, A., and McAuliffe, J. D. (2017). Variational inference: A review for statisticians. *Journal of the American statistical Association*, 112(518):859–877.

Bornn, L., Pillai, N. S., Smith, A., and Woodard, D. (2017). The use of a single pseudo-sample in approximate bayesian computation. *Statistics and Computing*, 27:583–590.

Brehmer, J., Louppe, G., Pavez, J., and Cranmer, K. (2020). Mining gold from implicit models to improve likelihood-free inference. *Proceedings of the National Academy of Sciences*, 117(10):5242–5249.

Cai, T. T., Wang, Y., and Zhang, L. (2021). The cost of privacy: Optimal rates of convergence for parameter estimation with differential privacy. *The Annals of Statistics*, 49(5):2825–2850.

Carroll, R. J., Ruppert, D., and Stefanski, L. A. (1995). *Measurement error in nonlinear models*, volume 105. CRC press.

Chaudhuri, K., Sarwate, A. D., and Sinha, K. (2013). A near-optimal algorithm for differentially-private principal components. *Journal of Machine Learning Research*, 14.

Covington, C., He, X., Honaker, J., and Kamath, G. (2021). Unbiased statistical estimation and valid confidence intervals under differential privacy. *arXiv preprint arXiv:2110.14465*.

Cranmer, K., Brehmer, J., and Louppe, G. (2020). The frontier of simulation-based inference. *Proceedings of the National Academy of Sciences*, 117(48):30055–30062.

Dinh, L., Sohl-Dickstein, J., and Bengio, S. (2016). Density estimation using real nvp. *arXiv preprint arXiv:1605.08803*.

Dong, J., Roth, A., and Su, W. J. (2022). Gaussian differential privacy. *Journal of the Royal Statistical Society Series B: Statistical Methodology*, 84(1):3–37.

Drechsler, J. (2023). Differential privacy for government agencies—are we there yet? *Journal of the American Statistical Association*, 118(541):761–773.

Durkan, C., Bekasov, A., Murray, I., and Papamakarios, G. (2019). Neural spline flows. *Advances in neural information processing systems*, 32.

Dwork, C., McSherry, F., Nissim, K., and Smith, A. (2006). Calibrating noise to sensitivity in private data analysis. In *Theory of Cryptography: Third Theory of Cryptography Conference, TCC 2006, New York, NY, USA, March 4-7, 2006. Proceedings 3*, pages 265–284. Springer.

Eisenberg, J. (2020). R0: How scientists quantify the intensity of an outbreak like coronavirus and its pandemic potential. <https://sph.umich.edu/pursuit/2020posts/how-scientists-quantify-outbreaks.html>. Accessed: 2023-10-08.

Evans, G. and King, G. (2023). Statistically valid inferences from differentially private data releases, with application to the facebook urls dataset. *Political Analysis*, 31(1):1–21.

Evans, G., King, G., Schwenzfeier, M., and Thakurta, A. (2019). Statistically valid inferences from privacy-protected data. *American Political Science Review*, pages 1–16.

Giddens, S. and Liu, F. (2023). *DPpack: Differentially Private Statistical Analysis and Machine Learning*. R package, Version 0.1.0.

Gillespie, D. T. (1977). Exact stochastic simulation of coupled chemical reactions. *The Journal of Physical Chemistry*, 81(25):2340–2361.

Gong, R. (2022). Exact inference with approximate computation for differentially private data via perturbations. *Journal of Privacy and Confidentiality*, 12(2).

Gong, R., Groshen, E. L., and Vadhan, S. (2022). Harnessing the known unknowns: Differential privacy and the 2020 census (co-editors' forward). *Harvard Data Science Review*, (Special Issue 2).

Gourieroux, C., Monfort, A., and Renault, E. (1993). Indirect inference. *Journal of applied econometrics*, 8(S1):S85–S118.

Greenberg, D., Nonnenmacher, M., and Macke, J. (2019). Automatic posterior transformation for likelihood-free inference. In *International Conference on Machine Learning*, pages 2404–2414. PMLR.

Gretton, A., Borgwardt, K. M., Rasch, M. J., Schölkopf, B., and Smola, A. (2012). A kernel two-sample test. *The Journal of Machine Learning Research*, 13(1):723–773.

Hu, Z., Ke, Z. T., and Liu, J. S. (2022). Measurement error models: from nonparametric methods to deep neural networks. *Statistical Science*, 37(4):473–493.

Ju, N., Awan, J., Gong, R., and Rao, V. (2022). Data augmentation mcmc for bayesian inference from privatized data. *Advances in neural information processing systems*, 35:12732–12743.

Karwa, V., Kifer, D., and Slavković, A. B. (2015). Private posterior distributions from variational approximations. *arXiv preprint arXiv:1511.07896*.

Kingma, D. P. and Ba, J. (2014). Adam: A method for stochastic optimization. *arXiv preprint arXiv:1412.6980*.

Kobyzev, I., Prince, S. J., and Brubaker, M. A. (2020). Normalizing flows: An introduction and review of current methods. *IEEE transactions on pattern analysis and machine intelligence*, 43(11):3964–3979.

Li, S., Zhang, L., Cai, T. T., and Li, H. (2023). Estimation and inference for high-dimensional generalized linear models with knowledge transfer. *Journal of the American Statistical Association*, pages 1–12.

Liu, F. (2018). Generalized gaussian mechanism for differential privacy. *IEEE Transactions on Knowledge and Data Engineering*, 31(4):747–756.

Lopez-Paz, D. and Oquab, M. (2016). Revisiting classifier two-sample tests. *arXiv preprint arXiv:1610.06545*.

Lueckmann, J.-M., Boelts, J., Greenberg, D., Goncalves, P., and Macke, J. (2021). Benchmarking simulation-based inference. In *International Conference on Artificial Intelligence and Statistics*, pages 343–351. PMLR.

Lueckmann, J.-M., Goncalves, P. J., Bassetto, G., Öcal, K., Nonnenmacher, M., and Macke, J. H. (2017). Flexible statistical inference for mechanistic models of neural dynamics. *Advances in neural information processing systems*, 30.

L'Ecuyer, P. (2018). *Randomized quasi-Monte Carlo: An introduction for practitioners*. Springer.

Miller, B. K., Weniger, C., and Forré, P. (2022). Contrastive Neural Ratio Estimation. *arXiv preprint arXiv:2210.06170*.

Nissim, K., Raskhodnikova, S., and Smith, A. (2007). Smooth sensitivity and sampling in private data analysis. In *Proceedings of the Thirty-Ninth Annual ACM Symposium on Theory of Computing*, STOC '07, page 75–84, New York, NY, USA. Association for Computing Machinery.

Owen, A. B. (1997). Monte carlo variance of scrambled net quadrature. *SIAM Journal on Numerical Analysis*, 34(5):1884–1910.

Papamakarios, G. and Murray, I. (2016). Fast  $\varepsilon$ -free inference of simulation models with bayesian conditional density estimation. *Advances in neural information processing systems*, 29.

Papamakarios, G., Nalisnick, E., Rezende, D. J., Mohamed, S., and Lakshminarayanan, B. (2021). Normalizing flows for probabilistic modeling and inference. *J. Mach. Learn. Res.*, 22(1).

Papamakarios, G., Pavlakou, T., and Murray, I. (2017). Masked autoregressive flow for density estimation. *Advances in neural information processing systems*, 30.

Papamakarios, G., Sterratt, D., and Murray, I. (2019). Sequential neural likelihood: Fast likelihood-free inference with autoregressive flows. In *The 22nd International Conference on Artificial Intelligence and Statistics*, pages 837–848. PMLR.

Rho, S., Cummings, R., and Misra, V. (2023). Differentially private synthetic control. In *International Conference on Artificial Intelligence and Statistics*, pages 1457–1491. PMLR.

Su, B., Wang, Y., Schiavazzi, D. E., and Liu, F. (2023). Differentially private normalizing flows for density estimation, data synthesis, and variational inference with application to electronic health records. *arXiv preprint arXiv:2302.05787*.

Waites, C. and Cummings, R. (2021). Differentially private normalizing flows for privacy-preserving density estimation. In *Proceedings of the 2021 AAAI/ACM Conference on AI, Ethics, and Society*, AIES ’21, page 1000–1009, New York, NY, USA. Association for Computing Machinery.

**Supplementary Materials to  
'Conditional Density Estimations from Privacy-Protected Data'**

## S1 Derivations for SPLE and SPPE objectives

**Lemma 5.** *For private data likelihood estimation, minimizing the average KL divergence  $\mathcal{D}_{\text{KL}}(p(s_{\text{dp}} | \theta) \| q_{\phi}(s_{\text{dp}} | \theta))$  under the prior  $p(\theta)$ , is equivalent to minimizing the objective function*

$$\ell_{\text{PLE}}(\phi) = \mathbb{E}_{p(\theta, x)} \left[ - \int_{\mathbb{S}} \eta(s_{\text{dp}} | x) \log q_{\phi}(s_{\text{dp}} | \theta) ds_{\text{dp}} \right]. \quad (\text{S1})$$

*With respect to the joint distribution  $\tilde{p}(\theta, x) \propto \tilde{p}(\theta) f(x | \theta)$ , the objective function still has the form*

$$\ell_{\text{PLE}}(\phi) = \mathbb{E}_{\tilde{p}(\theta, x)} \left[ - \int_{\mathbb{S}} \eta(s_{\text{dp}} | x) \log q_{\phi}(s_{\text{dp}} | \theta) ds_{\text{dp}} \right]. \quad (\text{S2})$$

*Proof.* Note that

$$\begin{aligned} & \mathbb{E}_{p(\theta)} [\mathcal{D}_{\text{KL}}(p(s_{\text{dp}} | \theta) \| q_{\phi}(s_{\text{dp}} | \theta))] \\ &= \int_{\Theta} p(\theta) \left[ \int_{\mathbb{S}} p(s_{\text{dp}} | \theta) (\log p(s_{\text{dp}} | \theta) - \log q_{\phi}(s_{\text{dp}} | \theta)) ds_{\text{dp}} \right] d\theta \\ &= C_1 - \iint_{\mathbb{S} \times \Theta} p(\theta) p(s_{\text{dp}} | \theta) \log q_{\phi}(s_{\text{dp}} | \theta) ds_{\text{dp}} d\theta \\ &= C_1 - \iiint_{\mathbb{S} \times \Theta \times \mathbb{X}^n} p(\theta) \eta(s_{\text{dp}} | x) f(x | \theta) \log q_{\phi}(s_{\text{dp}} | \theta) ds_{\text{dp}} d\theta dx \\ &= C_1 - \iint_{\Theta \times \mathbb{X}^n} p(\theta, x) \left[ \int_{\mathbb{S}} \eta(s_{\text{dp}} | x) \log q_{\phi}(s_{\text{dp}} | \theta) ds_{\text{dp}} \right] d\theta dx \\ &= C_1 - \mathbb{E}_{p(\theta, x)} \left[ \int_{\mathbb{S}} \eta(s_{\text{dp}} | x) \log q_{\phi}(s_{\text{dp}} | \theta) ds_{\text{dp}} \right], \end{aligned}$$

where  $C_1 = \iint_{\mathbb{S} \times \Theta} p(\theta) p(s_{\text{dp}} | \theta) \log p(s_{\text{dp}} | \theta) ds_{\text{dp}} d\theta$  is a constant unrelated to  $\phi$ . Furthermore, if  $\theta$  are sampled from some proposal  $\tilde{p}(\theta)$ , we still have

$$\begin{aligned} & \mathbb{E}_{\tilde{p}(\theta)} [\mathcal{D}_{\text{KL}}(p(s_{\text{dp}} | \theta) \| q_{\phi}(s_{\text{dp}} | \theta))] \\ &= \iint_{\mathbb{S} \times \Theta} \tilde{p}(\theta) p(s_{\text{dp}} | \theta) \log p(s_{\text{dp}} | \theta) ds_{\text{dp}} d\theta - \mathbb{E}_{\tilde{p}(\theta, x)} \left[ \int_{\mathbb{S}} \eta(s_{\text{dp}} | x) \log q_{\phi}(s_{\text{dp}} | \theta) ds_{\text{dp}} \right]. \end{aligned}$$

□

**Lemma 6.** *For private data posterior estimation, minimizing the average KL divergence  $\mathcal{D}_{\text{KL}}(p(\theta | s_{\text{dp}}) \| q_{\phi}(\theta | s_{\text{dp}}))$  with respect to the marginal evidence  $p(s_{\text{dp}}) = \int_{\mathbb{S}} p(\theta) p(s_{\text{dp}} | \theta) d\theta$ , is equivalent to minimizing the objective function*

$$\ell_{\text{PPE}}(\phi) = \mathbb{E}_{p(\theta, x)} \left[ - \int_{\mathbb{S}} \eta(s_{\text{dp}} | x) \log q_{\phi}(\theta | s_{\text{dp}}) ds_{\text{dp}} \right]. \quad (\text{S3})$$

*With respect to the joint distribution  $\tilde{p}(\theta, x) \propto \tilde{p}(\theta) f(x | \theta)$ , then the objective function has the form*

$$\ell_{\text{PPE-A}}(\phi) = \mathbb{E}_{\tilde{p}(\theta, x)} \left[ - \int_{\mathbb{S}} \eta(s_{\text{dp}} | x) \log \tilde{q}_{\phi}(\theta | s_{\text{dp}}) ds_{\text{dp}} \right], \quad (\text{S4})$$

*where*

$$\tilde{q}_{\phi}(\theta | s_{\text{dp}}) := q_{\phi}(\theta | s_{\text{dp}}) \frac{\tilde{p}(\theta)}{p(\theta)} \frac{1}{Z(s_{\text{dp}}, \phi)}, \quad Z(s_{\text{dp}}, \phi) = \int_{\Theta} q_{\phi}(\theta | s_{\text{dp}}) \frac{\tilde{p}(\theta)}{p(\theta)} d\theta.$$

*Proof.* We have

$$\begin{aligned}
& \mathbb{E}_{p(s_{dp})} [\mathcal{D}_{KL} (\pi(\theta | s_{dp}) \| q_\phi(\theta | s_{dp}))] \\
&= \int_{\mathbb{S}} p(s_{dp}) \left[ \int_{\Theta} \pi(\theta | s_{dp}) (\log \pi(\theta | s_{dp}) - \log q_\phi(\theta | s_{dp})) d\theta \right] ds_{dp} \\
&= C_2 - \iint_{\mathbb{S} \times \Theta} p(s_{dp}) \pi(\theta | s_{dp}) \log q_\phi(\theta | s_{dp}) ds_{dp} d\theta \\
&= C_2 - \iiint_{\mathbb{S} \times \Theta \times \mathbb{X}^n} p(\theta) \eta(s_{dp} | x) f(x | \theta) \log q_\phi(\theta | s_{dp}) ds_{dp} d\theta dx \\
&= C_2 - \iint_{\Theta \times \mathbb{X}^n} p(\theta, x) \left[ \int_{\mathbb{S}} \eta(s_{dp} | x) \log q_\phi(\theta | s_{dp}) ds_{dp} \right] d\theta dx \\
&= C_2 - \mathbb{E}_{p(\theta, x)} \left[ \int_{\mathbb{S}} \eta(s_{dp} | x) \log q_\phi(\theta | s_{dp}) ds_{dp} \right],
\end{aligned}$$

where  $C_2 = \iint_{\mathbb{S} \times \Theta} p(s_{dp}) \pi(\theta | s_{dp}) \log \pi(\theta | s_{dp}) ds_{dp} d\theta$  is a constant unrelated to  $\phi$ . Furthermore, if  $\theta$  are sampled from some proposal  $\tilde{p}(\theta)$ , then

$$\begin{aligned}
& \mathbb{E}_{p(s_{dp})} [\mathcal{D}_{KL} (\tilde{\pi}(\theta | s_{dp}) \| \tilde{q}_\phi(\theta | s_{dp}))] \\
&= \iint_{\mathbb{S} \times \Theta} p(s_{dp}) \tilde{\pi}(\theta | s_{dp}) \log \tilde{\pi}(\theta | s_{dp}) ds_{dp} d\theta - \mathbb{E}_{\tilde{p}(\theta, x)} \left[ \int_{\mathbb{S}} \eta(s_{dp} | x) \log \tilde{q}_\phi(\theta | s_{dp}) ds_{dp} \right], \quad (S5)
\end{aligned}$$

where  $\tilde{\pi}(\theta | s_{dp})$  is called *proposal posterior* (Greenberg et al., 2019), which satisfied

$$\tilde{\pi}(\theta | s_{dp}) = \pi(\theta | s_{dp}) \frac{\tilde{p}(\theta) p(s_{dp})}{\tilde{p}(\theta) \tilde{p}(s_{dp})}, \quad \tilde{p}(s_{dp}) = \int_{\Theta} \tilde{p}(\theta) p(s_{dp} | \theta) d\theta.$$

Based on Prop. 1 in the work of Papamakarios and Murray (2016), minimizing (S5) results in the convergence of  $\tilde{q}_\phi(\theta | s_{dp})$  to  $\tilde{\pi}(\theta | s_{dp})$  and  $q_\phi(\theta | s_{dp})$  to  $\pi(\theta | s_{dp})$ .  $\square$

## S2 Proof of Proposition 4

**Proposition 4.** Consider a sequence of  $L$  points in the time interval  $[0, T]$ , our privatized query can be  $s_{dp} = (s_1, \dots, s_L)$  where each  $s_i \sim \text{Binomial} \left( n, \frac{I(t_i) + m}{K + 2m} \right)$  independently. The mechanism generating  $s_{dp} = (s_1, \dots, s_L)$  satisfies  $\epsilon$ -DP, with  $\epsilon = \frac{n}{m}L$ .

*Proof.* Denote the numbers of infectious as  $I(t) \in \{0, 1, \dots, K\}$  and its neighbors  $\tilde{I}(t)$ , note that  $|I(t) - \tilde{I}(t)| \leq 1$  holds for all  $t \in [0, T]$  because a change of the infection status of any one of the  $K$  individuals will at most increase or decrease  $I(t)$  by only 1. We examine the following density ratio:

$$\begin{aligned}
\frac{p(s_i | I(t_i))}{p(s_i | \tilde{I}(t_i))} &= \frac{\binom{n}{s_i} \left( \frac{I(t_i) + m}{K + 2m} \right)^{s_i} \left( \frac{K - I(t_i) + m}{K + 2m} \right)^{(n - s_i)}}{\binom{n}{s_i} \left( \frac{\tilde{I}(t_i) + m}{K + 2m} \right)^{s_i} \left( \frac{K - \tilde{I}(t_i) + m}{K + 2m} \right)^{(n - s_i)}} \\
&= \left( \frac{I(t_i) + m}{\tilde{I}(t_i) + m} \right)^{s_i} \left( \frac{K - I(t_i) + m}{K - \tilde{I}(t_i) + m} \right)^{(n - s_i)} \\
&:= H_i.
\end{aligned}$$

This expression can be analyzed under three distinct cases. In the first case, when  $\tilde{I}(t_i) > I(t_i)$ , we have  $\tilde{I}(t_i) = I(t_i) + 1$ , leading to  $H_i \leq \left( \frac{K - I(t_i) + m}{K - \tilde{I}(t_i) + m} \right)^{(n - s_i)} \leq \left( \frac{K - I(t_i) + m}{K - I(t_i) + m} \right)^n \leq \left( \frac{1 + m}{m} \right)^n$ .

In the second case, if  $\tilde{I}(t_i) < I(t_i)$ , then  $\tilde{I}(t_i) = I(t_i) - 1$ , and we obtain  $H_i \leq \left(\frac{I(t_i)+m}{\tilde{I}(t_i)+m}\right)^{s_i} \leq \left(\frac{I(t_i)+m}{\tilde{I}(t_i)+m}\right)^n \leq \left(\frac{1+m}{m}\right)^n$ . Lastly, when  $\tilde{I}(t_i) = I(t_i)$ ,  $H_i$  equals to 1. Thus,  $\frac{p(s_i|I(t_i))}{p(s_i|\tilde{I}(t_i))} \leq \left(\frac{1+m}{m}\right)^n \leq \exp\left(\frac{n}{m}\right)$ . Now for  $s_{\text{dp}} = (s_1, \dots, s_L)$ , we have

$$\frac{p(s_{\text{dp}} | \{I(t) | t \in [0, T]\})}{p(s_{\text{dp}} | \{\tilde{I}(t) | t \in [0, T]\})} = \frac{p(s_{\text{dp}} | I(t_1), \dots, I(t_L))}{p(s_{\text{dp}} | \tilde{I}(t_1), \dots, \tilde{I}(t_L))} \leq \exp\left(\frac{n}{m}L\right),$$

which gives the mechanism generating  $s_{\text{dp}} = (s_1, \dots, s_L)$  satisfies  $\epsilon$ -DP, with  $\epsilon = \frac{n}{m}L$ .  $\square$

## S3 Experimental details

The training and inference processes of the methods were primarily implemented using the Pytorch package in Python.

**Experimental setup.** We employed neural spline flows (Durkan et al., 2019) as the conditional density estimator, consisting of 8 layers. Each layer was constructed using two residual blocks with 50 units and ReLU activation function, with 10 bins in each monotonic piecewise rational-quadratic transforms and the tail bound was set to 5.

In the training process, the number of samples simulated in each round is  $N = 1000$  and there are  $R = 10$  rounds in total. In each round of training, we randomly select 5% of the newly generated samples as validation data. According to the early stop criterion proposed by Papamakarios et al. (2019), we stop training if the value of loss on validation data does not increase after 20 epochs in a single round. For stochastic gradient descent optimizer, we choose the Adam (Kingma and Ba, 2014) with the batchsize of 100, the learning rate of  $5 \times 10^{-4}$  and the weight decay is  $10^{-4}$ .

### S3.1 SIR model

#### S3.1.1 Detailed results on synthetic data

In our experiments, we use the Gillespie algorithm (Gillespie, 1977) to simulate the whole process over a duration of  $T = 160$  time units, and recorded the populations at intervals of 1 time units. The prior distribution of  $\beta$  is set to  $\mathcal{N}(\log 0.4, 0.5)$  and prior distribution of  $\gamma$  is set to  $\mathcal{N}(\log 0.125, 0.2)$ . The value of  $K$  is configured as 1000000, while  $N$  is set to 1000 for the number of observations.

To publish the privatized data about the infection process, we select the infectious group  $I(t)$  at  $L = 10$  evenly-spaced points in time  $[0, T]$ , with the privacy parameters set to  $n = 1000$  and  $m = 1000$ , which satisfied  $\epsilon$ -DP with  $\epsilon = 10$ . The ground truth parameters is

$$\theta^* = (\exp(-0.5), \exp(-3)),$$

and the observed private statistic  $s_{\text{dp}}^o$  simulated from the model with ground truth parameters  $\theta^*$  is

$$s_{\text{dp}}^o = (0.0010, 0.0310, 0.6140, 0.2630, 0.1230, 0.0470, 0.0180, 0.0090, 0.0050, 0.0030).$$

Figure S1 illustrates the convergence of the approximate posterior by SPPE and SPLE in each round, and compares our results with the SMC-ABC method, where we performed simulations up to  $5 \times 10^5$  times for the SMC-ABC method to generate the near exact ‘True’ posterior. Figure S2 depicts the results of the SMC-ABC method under the same performance metrics. Our method, after 10 rounds or  $10^4$  simulations, achieved similar performance as the SMC-ABC method with approximately  $10^5$  simulations.

Finally, we investigate the marginal posterior distributions  $\pi(\beta | s_{\text{dp}})$  and  $\pi(\gamma | s_{\text{dp}})$  in Figure S3, and conclude that SPPE and SPLE perform similarly well. In this example, the posterior approximated by SPPE is slightly more concentrated than those from SMC-ABC and SPLE.

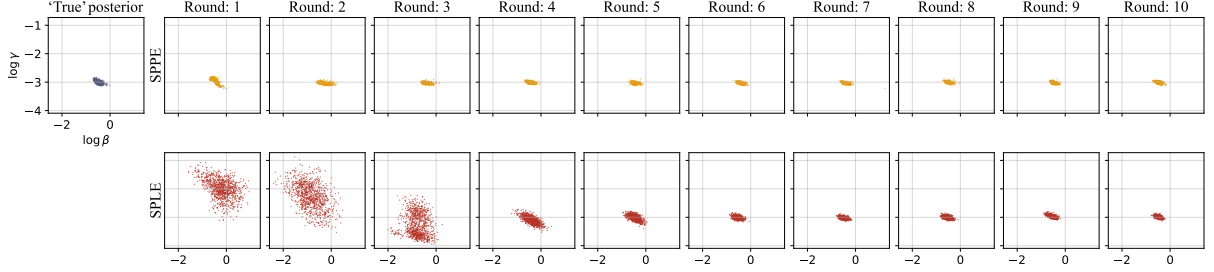


Figure S1: Detailed convergence of sequential posterior estimations given DP-protected infection trajectory under the SIR model. Each round entails  $N = 1000$  simulations. Orange: SPPE; red: SPLE; grey: SMC-ABC.

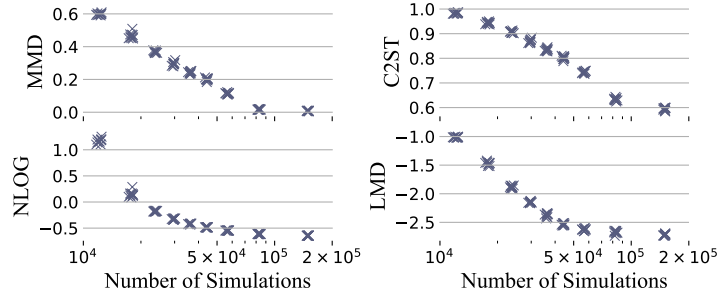


Figure S2: Approximation accuracy by SMC-ABC on the SIR model against number of simulations.

### S3.1.2 Inference on real disease outbreaks

We applied our inference methods (SPPE and SPLE) to analyze several real infectious disease outbreaks, namely influenza, Ebola, and Covid-19.

**influenza outbreak.** We utilized the dataset from a boarding school, obtained from <https://search.r-project.org/CRAN/refmans/epimdr/html/flu.html>. The total population in the school was  $K = 763$ . We considered a daily time interval, and the observed private statistic  $s_{dp}^o$  is

$$s_{dp, \text{flu}}^o = (0.0010, 0.0039, 0.0105, 0.0367, 0.0996, 0.2910, 0.3840, 0.3368, 0.3106, 0.2516).$$

**Ebola outbreak in West Africa, 2014.** We analyzed datasets from three regions: a) Guinea, b) Liberia, and c) Sierra Leone. The dataset source is from <https://usafacts.org/visualizations/coronavirus-covid-19-spread-map/state/nevada/county/clark-county/>. We assumed a potential contact individuals of  $K = 100,000$ . We selected 9 equally spaced time intervals of 120 days starting from 03/31/2014. The resulting observed private statistic  $s_{dp}^o$  is as follows

$$\begin{aligned} s_{dp,(a)}^o &= (0.0010, 0.0111, 0.0085, 0.0129, 0.0510, 0.0520, 0.0224, 0.0212, 0.0084, 0.0023). \\ s_{dp,(b)}^o &= (0.0010, 0.0007, 0.0019, 0.0664, 0.2579, 0.0742, 0.0610, 0.0542, 0.0172, 0.0003). \\ s_{dp,(c)}^o &= (0.0010, 0.0079, 0.0434, 0.2156, 0.2054, 0.0928, 0.0549, 0.0366, 0.0237, 0.0232). \end{aligned}$$

**Covid-19.** We examined the Covid-19 dataset for Clark County, Nevada. See <https://usafacts.org/visualizations/coronavirus-covid-19-spread-map/state/nevada/county/clark-county/>. We assumed a potential contact population of  $K = 100,000$ . We selected 9 equally spaced time intervals of 24 days, starting from 09/07/2020. To obtain the number of

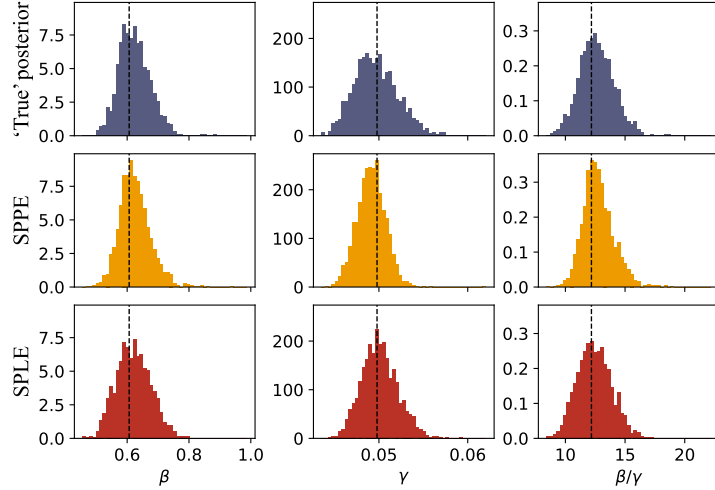


Figure S3: Marginal posterior histograms of  $\beta$ ,  $\gamma$ , and  $\beta/\gamma$  in SIR model on synthetic data. Grey: SMC-ABC; orange: SPPE; red: SPLE. The vertical lines indicate true data generating parameters, set to mimic a measles outbreak.

currently infected individuals, we calculated the difference in the total confirmed cases with a time interval of 14 days from the original dataset. The resulting observed private statistic  $s_{\text{dp}}^o$  is:

$$s_{\text{dp,covid}}^o = (0.0010, 0.0281, 0.0566, 0.0978, 0.2108, 0.2443, 0.2574, 0.0864, 0.0434, 0.0263).$$

The numerical results are presented and compared in Figure 4 of the main text.

### S3.2 Bayesian linear regression

**Data generating parameters.** Following the parameters settings in [Ju et al. \(2022\)](#), we model the predictors with  $x_{0,i} \sim \mathcal{N}_p(m, \Sigma)$ , where  $\Sigma = I_n$  and  $m = (0.9, -1.17)$ . The outcomes  $y$  satisfy  $y | x_0 \sim \mathcal{N}_n(x\beta, \sigma^2 I_n)$  where  $\sigma^2 = 2$ , and the prior for  $\beta$  is independent normal  $\mathcal{N}(0, 1)$ . We set the privacy loss budget  $\epsilon = 10$  and the number of subjects  $n = 100$ . The ground truth parameters are denoted as

$$\theta^* = (-1.79, -2.89, -0.66).$$

We simulate the summary statistics  $\tilde{s}$  from the model using the ground truth parameters  $\theta^*$ , resulting in

$$\tilde{s} = \left( \begin{pmatrix} -0.3742 \\ -0.0629 \\ 0.0299 \end{pmatrix}, 0.2499, \begin{pmatrix} 1.0000 & 0.0938 & -0.1270 \\ 0.0938 & 0.0180 & -0.0094 \\ -0.1270 & -0.0094 & 0.0280 \end{pmatrix} \right),$$

its corresponding vector form is

$$\tilde{s}_{\text{vec}} = (-0.3742, -0.0629, 0.0299, 0.2499, 0.0938, -0.1270, 0.0180, -0.0094, 0.0280).$$

Furthermore, the observed private statistic  $s_{\text{dp}}^o$  is given by

$$s_{\text{dp}}^o = \left( \begin{pmatrix} -0.3824 \\ -0.0667 \\ 0.0320 \end{pmatrix}, 0.2720, \begin{pmatrix} 1.0000 & 0.0988 & -0.1385 \\ 0.0988 & 0.0219 & -0.0229 \\ -0.1385 & -0.0229 & 0.0341 \end{pmatrix} \right),$$

its corresponding vector form is

$$s_{\text{dp,vec}}^o = (-0.3824, -0.0667, 0.0320, 0.2720, 0.0988, -0.1385, 0.0219, -0.0229, 0.0341).$$

**Experimental results.** In Figure S4, we present a comparison of the performance of the SPPE and SPLE methods across different metrics as the number of simulation rounds increases. The SPLE method demonstrates a faster convergence in this task. Figure S5 displays the posterior after 10 rounds, where both the SPPE and SPLE methods achieve results that are close to the near exact posterior obtained by the SMC-ABC method.

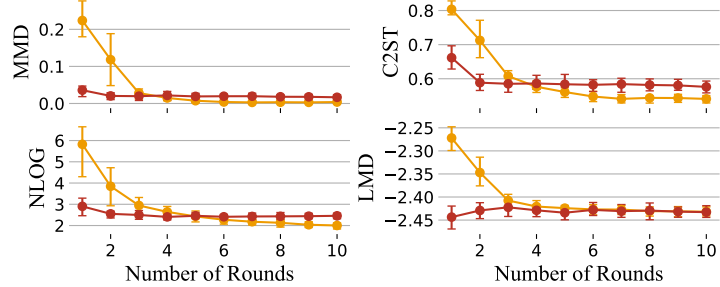


Figure S4: Approximation accuracy by SPPE (orange) and SPLE (red) on the Bayesian linear regression model against number of rounds, the error bars represent the mean with the upper and lower quartiles.

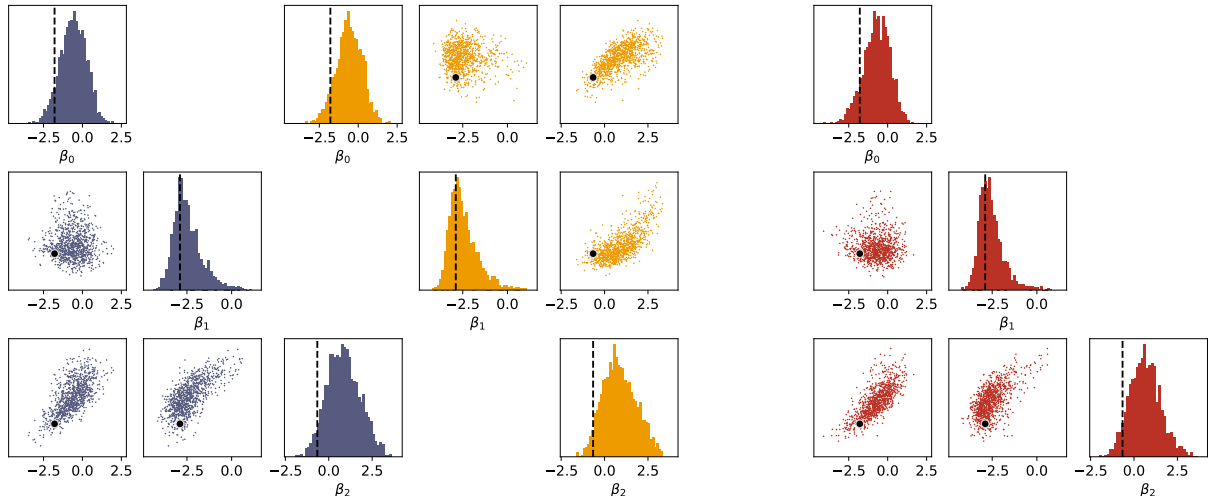


Figure S5: Posterior comparison on the Bayesian linear regression model. Grey: SMC-ABC; orange: SPPE; red: SPLE. The vertical lines and black dots indicate true data generating parameters.

### S3.3 Naïve Bayes log-linear model

**Model description.** The naïve Bayes log-linear model is a commonly used approach for modeling categorical data (Karwa et al., 2015). The input feature-vector, denoted as  $x = (x_1, \dots, x_K)$ , consists of  $K$  features, each taking values in the range  $\{1, 2, \dots, J_k\}$ . The output class, denoted as  $y$ , represents the target category and takes values in  $\{1, 2, \dots, I\}$ . The model assumes that the conditional probability of the input given the output, denoted as  $p(x \mid y)$ , can be factorized as the product of individual feature probabilities:  $p(x \mid y) = \prod_{k=1}^K p(x_k \mid y)$ . The model parameters are  $p_{ij}^k$ , which represents the probability  $p(x_k = j \mid y = i)$ , with prior  $(p_{i,1}^k, \dots, p_{i,J_k}^k) \sim \text{Dirichlet}(\alpha_{i,1}^k, \dots, \alpha_{i,J_k}^k)$  for all  $i$  and  $k$ ; and  $p_i = p(y = i)$ , with prior  $(p_1, \dots, p_I) \sim \text{Dirichlet}(\alpha_1, \dots, \alpha_I)$ .

We assume that  $(n_{i,1}^k, \dots, n_{i,J_k}^k) \sim \text{Multinomial}(n_i; p_{i,1}^k, \dots, p_{i,J_k}^k)$  for all  $i$  and  $k$  and  $(n_1, \dots, n_I) \sim \text{Multinomial}(n; p_1, \dots, p_I)$ . Here  $n_{i,j}^k$  represents the counts  $\#(y = i, x_k = j)$ . One sufficient

statistics of the model are the proportion of the counts  $r_{i,j}^k := \frac{1}{n} n_{i,j}^k$ , where  $n = \sum_{i=1}^I \sum_{j=1}^{J_k} n_{i,j}^k$  for all  $k$ . To protect the privacy of the dataset, Laplace noise  $e_{i,j}^k$  is added to the proportion of the counts, resulting in the privatized proportion  $m_{i,j}^k = r_{i,j}^k + e_{i,j}^k$ . When  $e_{i,j}^k \sim \text{Laplace}(0, \frac{2K}{n\epsilon})$ , the released private statistic  $\{m_{i,j}^k\}_{i,j,k}$  satisfied  $\epsilon$ -DP.

In our simulation, we set  $\alpha_{i,j}^k = \alpha_i = 2$  for all  $i, j, k$ , and  $n = 100$ , with  $I = 2$ ,  $K = 2$  and  $J_k = 2$  for all  $k$ . The privacy loss budget  $\epsilon = 10$ . The ground truth parameters are

$$\begin{aligned} p_{1,1}^1 &= 0.3887, \quad p_{1,2}^1 = 0.6113, \quad p_{1,1}^2 = 0.7537, \quad p_{1,2}^2 = 0.2463, \\ p_{2,1}^1 &= 0.6534, \quad p_{2,2}^1 = 0.3466, \quad p_{2,1}^2 = 0.5834, \quad p_{2,2}^2 = 0.4166, \\ p_1 &= 0.8489, \quad p_2 = 0.1511. \end{aligned}$$

and the observed private statistic simulated from the model with ground truth parameters are

$$\begin{aligned} r_{1,1}^1 &= 0.3275, \quad r_{1,2}^1 = 0.4520, \quad r_{1,1}^2 = 0.5862, \quad r_{1,2}^2 = 0.1827, \\ r_{2,1}^1 &= 0.1293, \quad r_{2,2}^1 = 0.0858, \quad r_{2,1}^2 = 0.1288, \quad r_{2,2}^2 = 0.0954. \end{aligned}$$

**Experimental results.** Figure S6 illustrates the performance of the SPPE and SPLE methods across four different metrics, and Figure S7 shows the marginal posterior histograms after 10 rounds, our methods stabilize in performance after round 3.

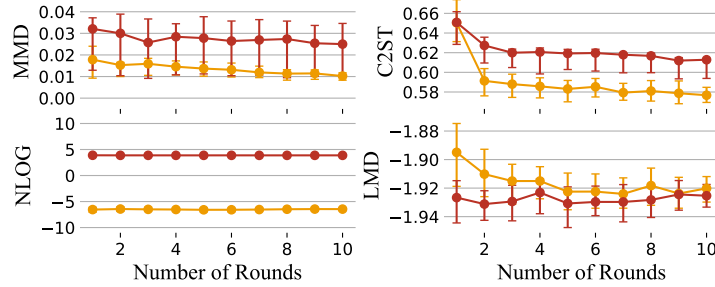


Figure S6: Approximation accuracy by SPPE (orange) and SPLE (red) on the log-linear model against number of rounds, the error bars represent the mean with the upper and lower quartiles.

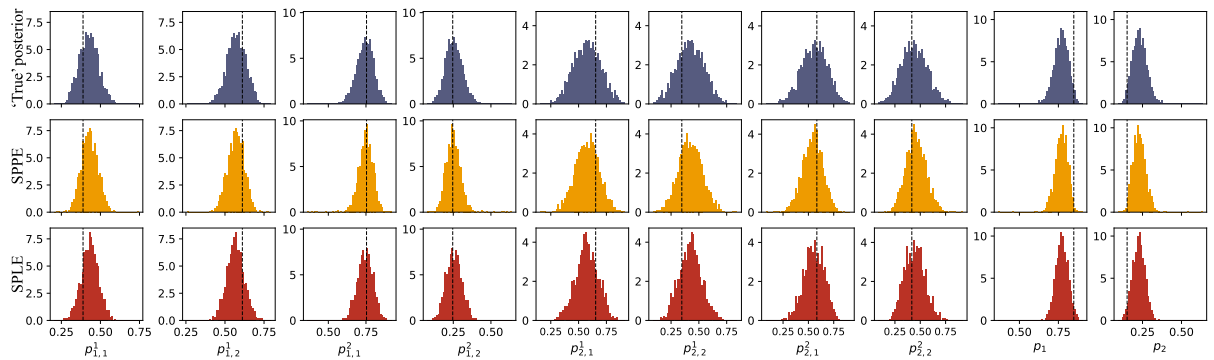


Figure S7: Marginal posterior histograms of the log-linear model. Grey: SMC-ABC; orange: SPPE; red: SPLE. The vertical lines indicate true data generating parameters.

## S4 Statement on Computing Resources

Our numerical experiments were conducted on a computer equipped with four GeForce RTX 2080 Ti graphics card and a pair of 14-core Intel E5-2690 v4 CPU.